



Numerical Simulations of Heavy Fermion Systems

L. C. Martin, F. F. Assaad, W. Hanke

published in

NIC Symposium 2008,
G. Münster, D. Wolf, M. Kremer (Editors),
John von Neumann Institute for Computing, Jülich,
NIC Series, Vol. **39**, ISBN 978-3-9810843-5-1, pp. 197-204, 2008.

© 2008 by John von Neumann Institute for Computing
Permission to make digital or hard copies of portions of this work for
personal or classroom use is granted provided that the copies are not
made or distributed for profit or commercial advantage and that copies
bear this notice and the full citation on the first page. To copy otherwise
requires prior specific permission by the publisher mentioned above.

<http://www.fz-juelich.de/nic-series/volume39>

Numerical Simulations of Heavy Fermion Systems

Lee C. Martin, Fakher F. Assaad, and Werner Hanke

Institut für Theoretische Physik und Astrophysik, Universität Würzburg
Am Hubland, 97074, Würzburg, Germany
E-mail: {*Lee.Martin, Fakher.Assaad, Werner.Hanke*}@*physik.uni-wuerzburg.de*

The Kondo lattice model describes a lattice of magnetic impurities embedded in a metallic host and is an appropriate starting point for the understanding of so-called heavy fermion systems. Those systems show a plethora of competing phases: a metallic Fermi-liquid state with effective mass exceeding by order of magnitudes the bare electron mass, magnetically ordered states as well as the coexistence of superconductivity and magnetism. Quantum phase transitions between the above mentioned phases as well as the mechanism triggering superconductivity remain unresolved issues of great interest in solid state physics. With the use of large scale numerical simulations in the framework of the Dynamical Cluster Approximation, we have investigated the evolution of the Fermi surface across the magnetic order-disorder transition. This is a central issue which lies at the heart of a theoretical understanding of this transition. Here we summarize our results which show a change in the topology of the Fermi surface across the transition thus supporting recent Hall effect experiments.

1 Introduction

In the 1960's the study of localized magnetic moments was placed firmly in the emerging field of strongly correlated electron systems when Anderson first identified interactions between localized electrons as the driving force for local moment formation¹. Early experimentalists realized that local moment formation on magnetic iron ions dissolved in non-magnetic metals is dependent on the host^{2,3}. The magnetic susceptibility of a system of iron dissolved in a niobium-molybdenum alloy was seen to follow a Curie-Weiss law for compositions close to molybdenum, indicating the presence of local moments. The low temperature limit of Curie-Weiss susceptibility is given by the Kondo temperature, the temperature at which the local moment is screened due to the formation of an entangled spin singlet state of the local moment and surrounding conduction electrons. Kondo physics lies in direct analogy to the phenomena of asymptotic freedom that governs quark physics. Like the quark, at high energies the local moment in the metallic host is free, but at energies below the Kondo temperature, it interacts so strongly with the surrounding electrons that it becomes screened or confined. The physics of local moment screening, manifests itself in a variety of properties of correlated electron systems including the Kondo resistivity minimum and also the formation of heavy fermion metals. With the latter, the presence of local moments greatly changes the metals properties with quasi-particles developing which may have an effective mass many times larger than the bare electron mass whilst still behaving as a Fermi liquid at low temperatures.

Such behaviour led Doniach to propose that the huge mass renormalization has its roots in a lattice version of the Kondo effect and that such heavy fermion systems should be modelled by the Kondo lattice model (KLM)⁴. The mass renormalization can be attributed to the coherent superposition of individual Kondo screening clouds and the resulting metallic state is characterized by a Fermi surface with Luttinger volume (Fermi surface volume)

containing both conduction and localized electrons. In its simplest form, the KLM describes a lattice of spin 1/2 magnetic moments coupled antiferromagnetically via an exchange coupling J to a single band of conduction electrons and is believed to capture the physics of heavy fermion materials such as CeCu_6 .

Although the physics of the single impurity Kondo problem is well understood⁵ the KLM still poses a problem half a century since its original conception. The difficulty with the lattice problem arises due to the presence of two competing energy scales. The first energy scale, given by the Kondo temperature, is associated with the screening of impurity spins via the Kondo effect. However, in the lattice problem, polarization of the conduction electron spins around a first magnetic impurity can couple to a second impurity leading to an effective interaction between impurity spins, the Ruderman-Kittel-Kasuya-Yosida (RKKY) interaction⁶⁻⁸, and an associated second energy scale. This RKKY scale dominates at low values of the exchange coupling and is the driving force for the observed magnetic order-disorder quantum phase transitions in heavy fermion materials. The nature of this phase transition is of current interest following experimental results suggesting a sudden change in the Fermi surface topology at the quantum critical point (QCP) for the heavy fermion metal YbRh_2Si_2 ⁹. Tuning this system from the non-magnetic heavy fermion metallic phase to the antiferromagnetic metallic phase causes a rapid change in the low temperature Hall coefficient which is extrapolated to a sudden jump at $T = 0$. Since the low-temperature Hall coefficient is related to the Fermi surface volume the results are interpreted as showing a sudden reordering of the Fermi surface at the QCP from a *large* Fermi surface, where the local moment impurity spins are included in the Luttinger volume, to a *small* Fermi surface where the impurity spins drop out of the Fermi surface volume.

This issue forms one of the central issues of our work. In this article we briefly present this and other recent results of our numerical simulations of the KLM and attempt to highlight the essential need for high performance computing in this project.

2 Numerical Solution of the Kondo Lattice Model

We take the KLM in two dimensions as our model heavy fermion system with Hamiltonian given by

$$H = \sum_{\mathbf{k}, \sigma} \epsilon(\mathbf{k}) c_{\mathbf{k}, \sigma}^\dagger c_{\mathbf{k}, \sigma} + J \sum_{\mathbf{i}} \mathbf{S}_{\mathbf{i}}^c \cdot \mathbf{S}_{\mathbf{i}}^f \quad (1)$$

with $c_{\mathbf{k}, \sigma}^\dagger$ creating a conduction electron on an extended orbital with wave vector \mathbf{k} and a z-component of spin $\sigma = \uparrow, \downarrow$. The spin 1/2 degrees of freedom, coupled via J , are represented with the aid of the Pauli spin matrices $\boldsymbol{\sigma}$ by $\mathbf{S}_{\mathbf{i}}^c = \frac{1}{2} \sum_{s, s'} c_{\mathbf{i}, s}^\dagger \boldsymbol{\sigma}_{s, s'} c_{\mathbf{i}, s'}$ or the equivalent definition for $\mathbf{S}_{\mathbf{i}}^f$ using the localized orbital creation operators $f_{\mathbf{i}, \sigma}^\dagger$. The KLM forbids charge fluctuations on the f -orbitals and as such the constraint of one electron per localized orbital must be included.

A numerical approach to solving the model is advantageous because such an approach will be non-biased. Due to the sheer size of the electron configuration (Hilbert) space of even a moderately small lattice of interacting electrons, exact solution methods, for example exact diagonalization, become impossible in practice. The quantum Monte Carlo

(QMC) approach stochastically samples the configuration space according to the statistical weight of a given configuration to arrive at an averaged solution with a statistical error dependant on the number of samples taken. However a common problem of QMC based simulations manifests itself as the minus sign problem in which the statistical weight of a sampled configuration may be negative. For a given algorithm the problem becomes severe if the average of this sign becomes small since then the number of stochastic samples required to give decent statistics increases exponentially. Previous QMC calculations of the KLM have been limited to finite sized lattices and in particular to particle-hole symmetry (half-filling) due to a severe minus sign problem.

In our project we examine the KLM in the hole-doped regime. We do this by employing the dynamical cluster approximation (DCA) in combination with a QMC algorithm for solving the model on the cluster.

3 The Dynamical Cluster Approximation with a Quantum Monte Carlo Cluster Solver

Within the DCA the original N -site lattice problem is approximated by a finite sized cluster of N_c sites embedded in a bath of the remaining electrons^{10,11}. Interactions within the cluster are calculated exactly, whereas interactions between the cluster and the bath are accounted for at a mean field level in space coordinates whilst retaining the full dynamics in imaginary time. The approximation will be particularly valid for systems in which spatial fluctuations are short-ranged. This equates to assuming only a weak momentum dependency of correlation functions. In momentum space the Brillouin zone is divided into N_c patches and strict momentum conservation is relaxed by only requiring conservation for transfers taking the \mathbf{k} -vector out of the patch.

Our implementation of the DCA does not suppress the development of antiferromagnetic order as is the case with a standard DCA approach. Broken symmetry is taken into consideration by defining a unit cell of two lattice sites containing, in total, two conduction electrons and two localized f-electron orbitals. This is the smallest cluster, which we denote by $N_c^{AF} = 1$, with which we can capture antiferromagnetic ordering and is the smallest cluster we consider in this article. Fig. 1 defines the basis vectors used, the unit cell and site indices within a cell. Allowing for antiferromagnetic ordering, translational symmetry is now only assumed for the new basis vectors \mathbf{a}_1 and \mathbf{a}_2 so that, in momentum space, the Brillouin zone is reduced to the magnetic Brillouin zone (MBZ). Patching of the MBZ is demonstrated in Fig. 1 for a cluster of size $N_c^{AF} = 4$. Importantly, the DCA self-consistent equation for the lattice Green function becomes a matrix equation since each site of the lattice defined by \mathbf{a}_1 and \mathbf{a}_2 is now a unit cell of four orbitals.

A basic requirement for using the DCA is the ability to effectively calculate the quantity $\Sigma^c[\bar{G}(\mathbf{K}, i\omega_n)]$, the self-energy on the cluster. In our work we achieve this via the QMC Hirsch-Fye impurity algorithm¹² proceeding as in Ref.¹³.

From a technical point of view the bulk of the numerical effort lies within the calculation of the self-energy on the cluster via the QMC impurity algorithm. Here the computational time scales with $(\beta N_c^{AF})^3$ where β is the inverse temperature. Even for a *small* cluster containing 16 orbitals the computational effort required to obtain decent statistics is immense. High performance computing is at this stage essential and, since QMC methods are easily parallelized, highly applicable. Additionally, we note that during a typical

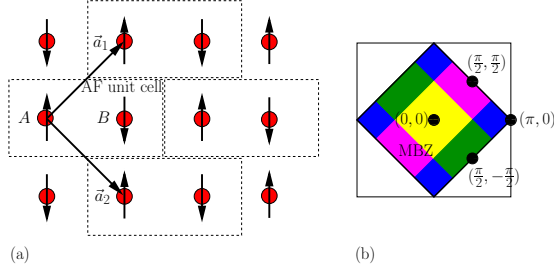


Figure 1. (a) Definition of the real space basis vectors, unit cell and orbital indices (b) The reduced Brillouin zone and k-space patching for a cluster with $N_c^{AF} = 4$

program run 90% of the time within the QMC algorithm is devoted to the calculation of outer products which may be achieved by using a BLAS library routine. The algorithm may therefore be highly optimized.

4 Results

As an initial test of our method we have carried out simulations at the particle-hole symmetric point ($t'/t = 0$ and $\langle n_c \rangle = 1$) and compared the results with previous lattice QMC simulations¹³.

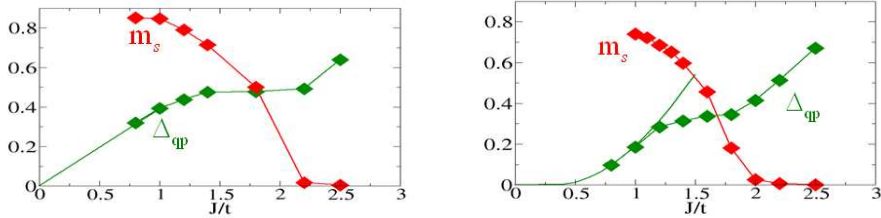


Figure 2. Left: DCA results for the staggered magnetization m_s and quasi-particle gap Δ_{qp} of the KLM at half-filling. Right: DCA results for the same quantities but now the model includes a next-nearest neighbour hopping term $t'/t = -0.3$

As shown in Fig. 2 (left side plot) the result for the staggered magnetization captures the phase transition from a paramagnetic to an antiferromagnetic phase with decreasing J/t . In addition, for small J/t the linear dependency of the quasi-particle gap, which appears in the results of Ref.¹³, is well reproduced with the DCA results. At half-filling the Fermi-surface exhibits perfect nesting, so to examine the influence of this on the magnetization and quasi-particle gap we deformed the Fermi-surface by introducing a frustration term into the Hamiltonian in the form of a nearest-neighbour hopping $t'/t = -0.3$. The results (Fig. 2, right) still demonstrate a magnetically ordered phase, now at lower critical J/t , but the linear behaviour of the quasi-particle gap is lost for small J/t and the gap now appears

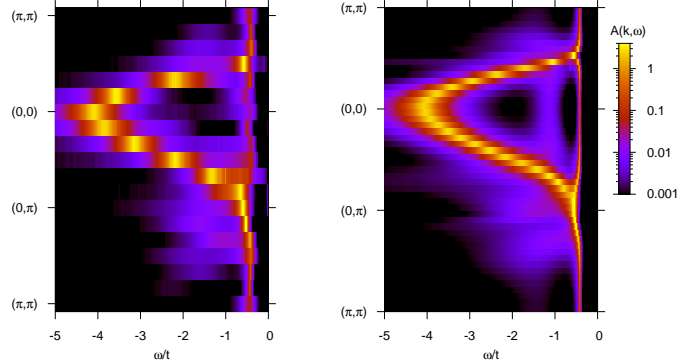


Figure 3. The single particle spectral function of the KLM at half-filling ($t'/t = 0$ and $\langle n_c \rangle = 1$) and with coupling $J/t = 1.2$ resulting from (left) a 12×12 -lattice QMC simulation using the projective auxiliary field algorithm of Ref.¹³ and (right) the DCA with cluster size $N_c^{AF} = 1$ and $\beta t = 40.0$

to follow a Kondo-scale, $\Delta_{qp}/t \propto e^{-W/J}$. This is an important result which concludes that a linear dependency of the quasi-particle gap is not generic to the system but rather is a direct consequence of particle-hole symmetry.

Initially remaining at half-filling we are able to show, by comparison of our band structure results with those of previous QMC calculations, that already a two-site cluster captures the key elements (Fig. 3). The parameters chosen for the plots are for an antiferromagnetic insulating point in the magnetic phase diagram. Although antiferromagnetic, the spectrum still retains a very flat heavy fermion band. This band, however, is then backfolded according to the symmetry effects introduced by the reduction of the Brillouin zone to a magnetic Brillouin zone as a direct result of antiferromagnetic ordering and breaking of the original translational symmetry. This behaviour is already well documented in the half-filled KLM, and the agreement of our results with those of previous studies confirms our belief that our DCA variant contains the necessary ingredients to investigate the delicate interplay between the RKKY interaction and Kondo physics.

In Fig. 4 we map out the ground state magnetic phase diagram of the KLM as a function of coupling J/t and conduction band hole-doping. Since we are interested in ground state properties the choice for the inverse temperature βt must be large enough to ensure we are below the smallest scale in the problem which will either be the coherence temperature or the RKKY scale. This requirement limits our simulations to the region $J/t \geq 0.8$ since the coherence scale decays exponentially with J/t and the computational time required by the QMC cluster solver scales as $(\beta N_c^{AF})^3$. Quite generally the onset of magnetism at small values of J/t is expected because the RKKY scale, set by $J^2 \chi(\mathbf{q}, \omega = 0)$, then dominates over the Kondo scale given by $T_K \sim e^{-t/J}$. We note that the sign problem which restricts pure QMC simulations to the particle-hole symmetric case is not severe within the DCA framework.

Having confirmed the existence of an antiferromagnetically ordered metallic phase we now address the issue of the Fermi surface topology. In Fig. 5 we show results for the single particle energy excitation spectrum for parameter points with constant coupling J/t but on either side of the quantum phase transition. The energies ω/t are plotted relative to

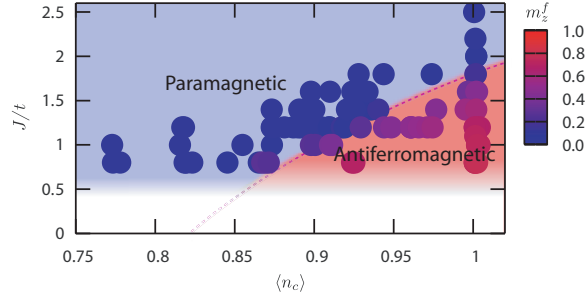


Figure 4. The magnetic phase diagram of the hole-doped KLM showing simulation results for the staggered magnetization m_z^f (colour-coded circles) as a function of coupling J/t and conduction electron occupancy $\langle n_c \rangle$. The shading of the antiferromagnetic and paramagnetic regions is intended only as a guide to the eye. We have included $t'/t = -0.3$ and the calculations are carried out with the $N_c^{AF} = 1$ cluster.

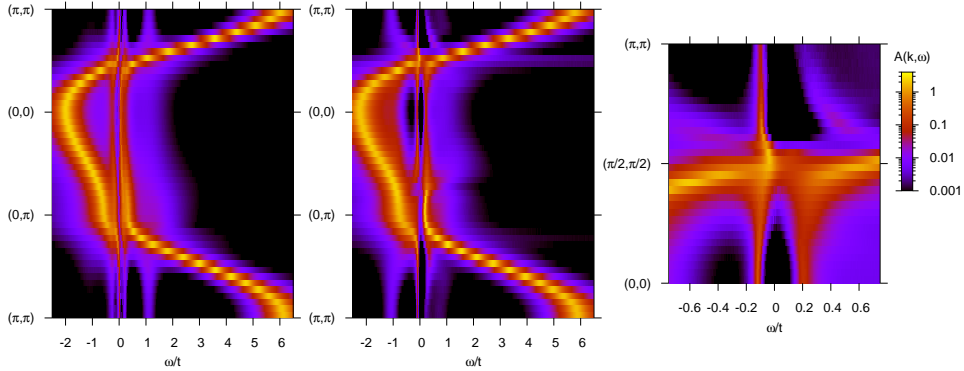


Figure 5. Left: DCA single particle spectrum for a simulation in the paramagnetic region ($J/t = 1.0$, $\langle n_c \rangle = 0.855$ and $\beta t = 40.0$). Centre: The spectrum of an antiferromagnetic point ($N_c^{AF} = 4$, $J/t = 1.0$, $\langle n_c \rangle = 0.977$ and $\beta t = 40.0$) across the phase transition but at the same coupling J/t . Right: Zoomed section of the central plot along the path $(0, 0)$ to (π, π) for energies around the Fermi energy

the Fermi energy and by observing where bands cross the Fermi energy we may deduce the topology of the Fermi surface. Beginning with the paramagnetic point the presence of very flat bands at the Fermi energy and around (π, π) , and therefore a large effective electron mass, is no surprise since this region of parameter space can be well understood by considering a simple large- N mean field approach. The Fermi surface in this case is given by the left hand plot in Fig. 6 with unoccupied states around (π, π) and equivalent points. In the antiferromagnetic case we note the continued existence of flat heavy fermion bands but also that these bands drop below the Fermi energy around (π, π) and give way instead to pockets of unoccupied states around $(\pi/2, \pi/2)$. The resultant Fermi surface is represented in the right hand plot of Fig. 6. Evidently, the development of antiferromagnetic order is related to a complete reordering of the Fermi surface. For a more detailed analysis of such issues as whether the Luttinger volume counts the impurity orbitals in each case and other

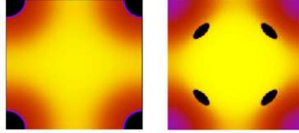


Figure 6. Depiction of the Fermi surface in the paramagnetic metallic state (left) and the antiferromagnetic metallic state (right)

related issues we refer the interested reader to our recent paper¹⁴.

5 Conclusions

In this article we have reported on our current progress towards understanding the hole-doped, two dimensional KLM ground state. The DCA approach is able to capture the delicate interplay between Kondo screening and magnetic ordering, as demonstrated by comparison with earlier finite lattice QMC data at half-filling but the DCA has the clear advantage in the doped region since the sign problem is not severe. The central result presented here is the change of topology in the Fermi surface — large Fermi surface to hole pockets — when the system is tuned through the magnetic transition. This result has profound implications on the theoretical understanding of the phase transition. It invalidates the generic Hertz-Millis approach which relies of a Fermi surface topology which remains unchanged through the transition^{15,16}, and calls for alternative descriptions^{17,18}. Clearly to pin down this important aspect, a more detailed investigation of the nature of the phase transition as well as the transition from one Fermi surface topology to the other in the region of the phase transition is required and ongoing. In parallel to this we are very interested in the effect of temperature on the single particle spectrum and work is also currently in progress to follow the evolution of the single particle excitation spectrum through different energy scales.

The statistically high quality data required to produce our current results and to achieve the above goals in the future, represents a significant investment in terms of computational cost. This ambitious project, which may be seen as a *grand challenge* in the field of correlated electron systems, would not be possible outside of the realms of high performance computing.

Acknowledgments

We would like to thank the Forschungszentrum Jülich for generous allocation of CPU time on the IBM Blue Gene/L and the DFG for financial support. We thank K. Beach, S. Capponi, S. Hochkeppel, T. C. Lang, T. Pruschke and M. Vojta for conversations.

References

1. P. W. Anderson, *Localized Magnetic States in Metals*, Phys. Rev., **124**, no. 1, 41–53, Oct 1961.

2. B. T. Matthias, M. Peter, H. J. Williams, A. M. Clogston, E. Corenzwit, and R. C. Sherwood, *Magnetic Moment of Transition Metal Atoms in Dilute Solution and Their Effect on Superconducting Transition Temperature*, Phys. Rev. Lett., **5**, no. 12, 542–544, Dec 1960.
3. A. M. Clogston, B. T. Matthias, M. Peter, H. J. Williams, E. Corenzwit, and R. C. Sherwood, *Local Magnetic Moment Associated with an Iron Atom Dissolved in Various Transition Metal Alloys*, Phys. Rev., **125**, no. 2, 541–552, Jan 1962.
4. S. Doniach, *The Kondo lattice and weak antiferromagnetism*, Physica B, **91**, 231–234, Jul 1977.
5. A. C. Hewson, *The Kondo Problem to Heavy Fermions*, Cambridge Studies in Magnetism. Cambridge University Press, Cambridge, 1997.
6. M. A. Ruderman and C. Kittel, *Indirect Exchange Coupling of Nuclear Magnetic Moments by Conduction Electrons*, Phys. Rev., **96**, no. 1, 99, Oct 1954.
7. Tadao Kasuya, *A Theory of Metallic Ferro- and Antiferromagnetism on Zener's Model*, Prog. Theo. Phys., **16**, no. 1, 45–57, 1956.
8. Kei Yosida, *Magnetic Properties of Cu-Mn Alloys*, Phys. Rev., **106**, no. 5, 893–898, Jun 1957.
9. S. Paschen, T. Lühmann, S. Wirth, P. Gegenwart, O. Trovarelli, C. Geibel, F. Steglich, P. Coleman, and Q. Si, *Hall-effect evolution across a heavy-fermion quantum critical point*, Nature, **432**, 881, 2004.
10. M. H. Hettler, M. Mukherjee, M. Jarrell, and H. R. Krishnamurthy, *Dynamical cluster approximation: Nonlocal dynamics of correlated electron systems*, Phys. Rev. B, **61**, 12739, 2000.
11. T. Maier, M. Jarrell, T. Pruschke, and M. H. Hettler, *Quantum cluster theories*, Rev. Mod. Phys., **77**, 1027, 2005.
12. J. E. Hirsch and R. M. Fye, *Monte Carlo Method for Magnetic Impurities in Metals*, Phys. Rev. Lett., **56**, no. 23, 2521–2524, Jun 1986.
13. S. Capponi and F. F. Assaad, *Spin and charge dynamics of the ferromagnetic and antiferromagnetic two-dimensional half-filled Kondo lattice model*, Phys. Rev. B, **63**, 155114, 2001.
14. L. C. Martin and F. F. Assaad, *Evolution of the Fermi Surface across a Magnetic Order-Disorder Transition in the Two-Dimensional Kondo Lattice Model: A Dynamical Cluster Approach*, 2007, arXiv:0711.2235 (submitted to Phys. Rev. Lett.).
15. John A. Hertz, *Quantum critical phenomena*, Phys. Rev. B, **14**, no. 3, 1165–1184, Aug 1976.
16. A. J. Millis, *Effect of a nonzero temperature on quantum critical points in itinerant fermion systems*, Phys. Rev. B, **48**, no. 10, 7183–7196, Sep 1993.
17. Q. Si, S. Rabello, K. Ingersent, and J.L. Smith, *Locally critical quantum phase transitions in strongly correlated metals.*, Nature, **413**, 804, 2001.
18. T. Senthil, Matthias Vojta, and Subir Sachdev, *Weak magnetism and non-Fermi liquids near heavy-fermion critical points*, Physical Review B (Condensed Matter and Materials Physics), **69**, no. 3, 035111, 2004.